Int. J. Appl. Math. Comput. Sci., 2020, Vol. 30, No. 4, 649–658
DOI: 10.34768/amcs-2020-0048

STABILITY ANALYSIS OF INTERCONNECTED DISCRETE–TIME FRACTIONAL–ORDER LTI STATE–SPACE SYSTEMS

ŁUKASZ GRZYMKOWSKI [a,*], DAMIAN TROFIMOWICZ [a], TOMASZ P. STEFAŃSKI [a]

[a] Faculty of Electronics, Telecommunications and Informatics
Gdańsk University of Technology
Narutowicza 11/12, 80-233 Gdańsk, Poland
e-mail: lukegrzym@gmail.com

In this paper, a stability analysis of interconnected discrete-time fractional-order (FO) linear time-invariant (LTI) state-space systems is presented. A new system is formed by interconnecting given FO systems using cascade, feedback, parallel interconnections. The stability requirement for such a system is that all zeros of a non-polynomial characteristic equation must be within the unit circle on the complex z-plane. The obtained theoretical results lead to a numerical test for stability evaluation of interconnected FO systems. It is based on modern root-finding techniques on the complex plane employing triangulation of the unit circle and Cauchy's argument principle. The developed numerical test is simple, intuitive and can be applied to a variety of systems. Furthermore, because it evaluates the function related to the characteristic equation on the complex plane, it does not require computation of state-matrix eigenvalues. The obtained numerical results confirm the efficiency of the developed test for the stability analysis of interconnected discrete-time FO LTI state-space systems.

Keywords: stability analysis, discrete-time systems, fractional-order systems.

1. Introduction

Stability is a fundamental problem in all branches of engineering. Any type of system, in the areas such as control engineering, signal processing, mechanical, civil or aerospace engineering, must be stable. In this paper, we focus on stability analysis of discrete-time linear time-invariant (LTI) systems. Such a classical system of integer order (IO) is (asymptotically) stable if and only if all zeros of the characteristic equation are within the unit circle on the complex z-plane (Ogata, 1987; Oppenheim *et al.*, 1999; Jury, 1964). An analogous criterion of stability also exists for fractional-order (FO) systems (Ostalczyk, 2012; Stanislawski and Latawiec 2013a; 2013b; Busłowicz and Kaczorek, 2009; Busłowicz and Ruszewski, 2013; Busłowicz, 2012). The main difference between the stability criteria for FO and IO systems relies in different shapes of stability contours on the complex z-plane. It stems from the fact that the characteristic equation is not a polynomial for FO systems. We have already addressed the issue of stability of a single discrete-time LTI system from a numerical point of view (Grzymkowski and Stefański, 2018b; 2018a).

Although the theory of FO systems has been a popular research topic recently (Bingi *et al.*, 2019; Kaczorek and Ruszewski, 2020), the stability of FO interconnected systems remains a subject that has not been thoroughly investigated yet to the best of our knowledge. Moreover, industrial applications of such systems have recently been reported (Mercorelli, 2017a; 2017b). We have thus decided to investigate basic interconnections (Vaccaro, 1995; Brogan, 1991) of two FO systems. Then, the results are generalized into more than two interconnected systems. The characteristic equation of interconnected FO systems is complicated and the stability cannot be easily evaluated using existing approaches. Therefore, we formulate a general numerical test for stability evaluation of systems, including interconnected systems, whose stability depends on the location of zeros of the non-polynomial characteristic equation.

The proposed method is based on an algorithm finding global complex roots and poles, employing triangulation and Cauchy's argument principle (Kowalczyk, 2018a). It allows for exploration of

*Corresponding author

various system models by analysing the characteristic equation $f(z) = 0$ which can include singular points and branch cuts. In the proposed method, the area outside the unit circle ($|z| = 1$) is transformed into its interior with the use of the inverse variable w (i.e., $z = w^{-1}$, $F(w) = f(w^{-1}) = 0$). Then, using triangulation, the obtained function is sampled within the unit circle and sign changes are detected for its real and imaginary parts separately. If the real and imaginary parts of the function change simultaneously signs for both ends of the same edge, then a zero of the function $F(w)$ can be located in its vicinity. The existence of the function zero is finally proved with the use of Cauchy's argument principle. Because the developed test evaluates a complex-valued function related to the characteristic equation on the complex plane, it does not require computation of eigenvalues. The obtained results confirm that the developed numerical test is an efficient tool for the stability analysis of interconnected discrete-time FO LTI state-space systems.

2. Stability condition for discrete-time FO LTI systems

Let us define two discrete-time FO LTI systems (which are considered in the paper) using the following state-space equations (Stanislawski and Latawiec, 2013a; 2013b):

$$\begin{aligned} \Delta^{\alpha}\mathbf{x}_1(n+1) &= \mathbf{A}_{f1}\mathbf{x}_1(n) + \mathbf{B}_1\mathbf{u}_1(n), \\ \mathbf{y}_1(n) &= \mathbf{C}_1\mathbf{x}_1(n) + \mathbf{D}_1\mathbf{u}_1(n), \end{aligned} \tag{1}$$

$$\begin{aligned} \Delta^{\beta}\mathbf{x}_2(n+1) &= \mathbf{A}_{f2}\mathbf{x}_2(n) + \mathbf{B}_2\mathbf{u}_2(n), \\ \mathbf{y}_2(n) &= \mathbf{C}_2\mathbf{x}_2(n) + \mathbf{D}_2\mathbf{u}_2(n). \end{aligned} \tag{2}$$

In (1) and (2), $n = 0, 1, \ldots$ denotes the discrete time, $\alpha, \beta \in (0, 2)$ denote FO values and $\mathbf{A}_{fi} = \mathbf{A}_i - \mathbf{I}$ ($i = 1, 2$) is the difference between the discrete-time state-space system matrix $\mathbf{A}_i$ and the identity matrix $\mathbf{I}$ being of the same dimension as $\mathbf{A}_i$. The dimensions of matrices $\mathbf{A}_1$ and $\mathbf{A}_2$ are N and M, respectively. Furthermore, $\mathbf{x}_i$, $\mathbf{u}_i$, $\mathbf{y}_i$ ($i = 1, 2$) respectively denote state, input and output vectors. The fractional difference is defined for discrete time as

$$\Delta^{\gamma}x(n) = \sum_{j=0}^{n}(-1)^j\binom{\gamma}{j}q^{-j}x(n), \tag{3}$$

where q^{-1} is the backward shift operator. The definition (3) directly results from the Grünwald-Letnikov difference of FO which is defined as (Samko *et al.*, 1993; Mozyrska and Girejko, 2013)

$$\Delta_T^{\gamma}f(t) = \sum_{j=0}^{\infty}(-1)^j\binom{\gamma}{j}f(t - jT), \tag{4}$$

where $\gamma > 0$ and the function f is defined on the real line. The definition (4) enables the Grünwald-Letnikov formulation of the (left-sided) derivative of the order $\gamma > 0$ given by (Samko *et al.*, 1993)

$$D^{\gamma}f(t) = \lim_{T\to 0^+}\frac{\Delta_T^{\gamma}f(t)}{T^{\gamma}}. \tag{5}$$

The expression (5) agrees with the usual derivative definition when γ is a positive integer.

Let us limit our considerations to a single FO system for a moment. For the system defined by (1), the characteristic equation in the $\mathcal{Z}$-transform domain is given by

$$f(z) = \det[z(1 - z^{-1})^{\alpha}\mathbf{I} - \mathbf{A}_{f1}] = 0. \tag{6}$$

The function $f(z)$ in the characteristic equation (6) can be considered as a polynomial of the complex variable $z(1 - z^{-1})^{\alpha}$. Hence, $f(z)$ has an infinite expansion into Laurent's series. For a discrete-time FO LTI system, the stability condition can be formulated in the following form.

Theorem 1. (Ostalczyk, 2012; Stanislawski and Latawiec, 2013a) *The discrete-time FO LTI system (1) with $\alpha \in (0, 2)$ is asymptotically stable if and only if all the roots of the characteristic equation* (6) *are strictly inside the unit circle on the complex z-plane.*

This means that the system (1) is unstable if at least a single zero of $f(z)$ exists outside the unit circle.

3. Interconnections of discrete-time FO LTI systems

Consider interconnected discrete-time FO LTI systems. For the sake of brevity, let us limit our considerations to basic interconnections of systems (1) and (2), which represent fundamental blocks for building any network of interconnected systems. That is, two systems (subsystems) are interconnected to form a single system. The obtained results can then be generalized towards any network of interconnected systems.

Consider the following state equations in the $\mathcal{Z}$-transform domain related respectively to the systems (1) and (2):

$$z(1 - z^{-1})^{\alpha}\mathbf{X}_1 = \mathbf{A}_{f1}\mathbf{X}_1 + \mathbf{B}_1\mathbf{U}_1, \tag{7}$$

$$z(1 - z^{-1})^{\beta}\mathbf{X}_2 = \mathbf{A}_{f2}\mathbf{X}_2 + \mathbf{B}_2\mathbf{U}_2. \tag{8}$$

From (3) it follows that

$$z(1 - z^{-1})^{\gamma} = \sum_{j=0}^{+\infty}(-1)^j\binom{\gamma}{j}z^{-j+1}, \tag{9}$$

where $\gamma = \alpha, \beta$. In general, the output equations related to (7) and (8) are respectively given by

$$\mathbf{Y}_1 = \mathbf{C}_1\mathbf{X}_1 + \mathbf{D}_1\mathbf{U}_1, \tag{10}$$

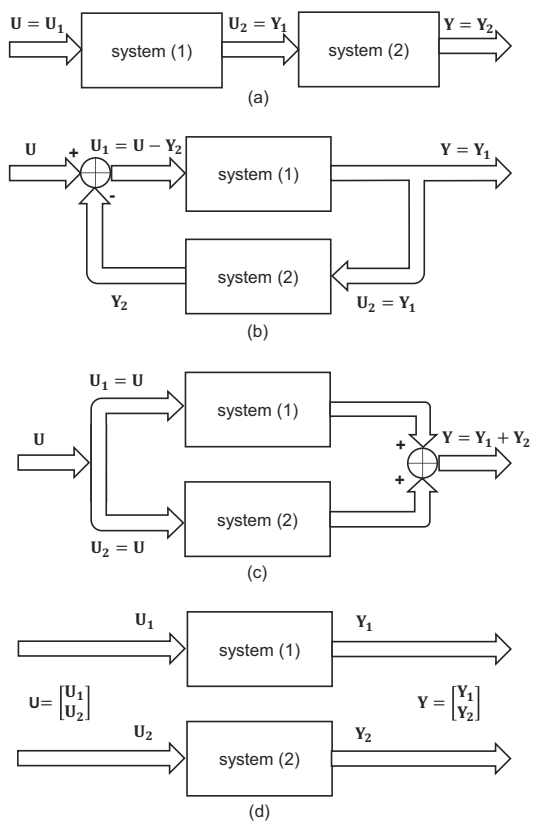

Fig. 1. Basic interconnections of two FO systems: cascade interconnection (a), feedback interconnection (b), parallel interconnection (c), isolated configuration with inputs and outputs appended (d).

$$\mathbf{Y}_2 = \mathbf{C}_2\mathbf{X}_2 + \mathbf{D}_2\mathbf{U}_2. \tag{11}$$

We assume that $\mathbf{D}_1 = \mathbf{D}_2 = 0$ for the sake of brevity.

In Fig. 1, four fundamental interconnections of two FO systems are presented: (a) cascade interconnection, (b) feedback interconnection, (c) parallel interconnection, and (d) isolated configuration with inputs and outputs appended.

3.1. Cascade interconnection. In this case, the output of the system (1) is the input to the system (2),

$$\mathbf{U}_2 = \mathbf{Y}_1, \tag{12}$$

whereas the output of the interconnected systems is given by (11). From (7), we obtain

$$\mathbf{X}_1 = \left[z(1-z^{-1})^{\alpha}\mathbf{I} - \mathbf{A}_{f1}\right]^{-1}\mathbf{B}_1\mathbf{U}_1. \tag{13}$$

Hence, based on (8), (10), (12) and (13),

$$\mathbf{X}_2 = \left[z(1-z^{-1})^{\beta}\mathbf{I} - \mathbf{A}_{f2}\right]^{-1}\mathbf{B}_2\mathbf{C}_1 \times \left[z(1-z^{-1})^{\alpha}\mathbf{I} - \mathbf{A}_{f1}\right]^{-1}\mathbf{B}_1\mathbf{U}_1, \tag{14}$$

accompanied by the output equation (11). The matrix which relates $\mathbf{X}_2$ and $\mathbf{U}_1$ in (14) is not a square matrix. Hence, (13) and (14) can be written as

$$\mathbf{M}_{cas}\begin{bmatrix}\mathbf{X}_1\\ \mathbf{X}_2\end{bmatrix} = \begin{bmatrix}\mathbf{B}_1\mathbf{U}\\ 0\end{bmatrix}, \tag{15}$$

where

$$\mathbf{M}_{cas} = \begin{bmatrix}z(1-z^{-1})^{\alpha}\mathbf{I} - \mathbf{A}_{f1} & 0\\ -\mathbf{B}_2\mathbf{C}_1 & z(1-z^{-1})^{\beta}\mathbf{I} - \mathbf{A}_{f2}\end{bmatrix}. \tag{16}$$

3.2. Feedback interconnection. For systems with the feedback loop, we get

$$\mathbf{U}_1 = \mathbf{U} - \mathbf{C}_2\mathbf{X}_2, \tag{17}$$

$$\mathbf{U}_2 = \mathbf{C}_1\mathbf{X}_1. \tag{18}$$

Applying (17) and (18) to (7) and (8), we see that

$$\mathbf{M}_{fl}\begin{bmatrix}\mathbf{X}_1\\ \mathbf{X}_2\end{bmatrix} = \begin{bmatrix}\mathbf{B}_1\mathbf{U}\\ 0\end{bmatrix}, \tag{19}$$

where

$$\mathbf{M}_{fl} = \begin{bmatrix}z(1-z^{-1})^{\alpha}\mathbf{I} - \mathbf{A}_{f1} & \mathbf{B}_1\mathbf{C}_2\\ -\mathbf{B}_2\mathbf{C}_1 & z(1-z^{-1})^{\beta}\mathbf{I} - \mathbf{A}_{f2}\end{bmatrix}. \tag{20}$$

3.3. Parallel interconnection. For the parallel interconnection of systems, the state equations (7) and (8) have the same input signal

$$\mathbf{U}_1 = \mathbf{U}_2 = \mathbf{U}, \tag{21}$$

whereas the output equation has the form

$$\mathbf{Y} = \mathbf{C}_1\mathbf{X}_1 + \mathbf{C}_2\mathbf{X}_2. \tag{22}$$

Combining (7), (8) and (21), we get

$$\mathbf{M}_{par}\begin{bmatrix}\mathbf{X}_1\\ \mathbf{X}_2\end{bmatrix} = \begin{bmatrix}\mathbf{B}_1\\ \mathbf{B}_2\end{bmatrix}\mathbf{U}, \tag{23}$$

where

$$\mathbf{M}_{par} = \begin{bmatrix}z(1-z^{-1})^{\alpha}\mathbf{I} - \mathbf{A}_{f1} & 0\\ 0 & z(1-z^{-1})^{\beta}\mathbf{I} - \mathbf{A}_{f2}\end{bmatrix}. \tag{24}$$

3.4. Isolated configuration with inputs and outputs appended. In this case, we consider simple mutually decoupled systems

$$\mathbf{M}_{app}\begin{bmatrix}\mathbf{X}_1\\ \mathbf{X}_2\end{bmatrix}=\begin{bmatrix}\mathbf{B}_1 & 0\\ 0 & \mathbf{B}_2\end{bmatrix}\begin{bmatrix}\mathbf{U}_1\\ \mathbf{U}_2\end{bmatrix}, \tag{25}$$

where

$$\mathbf{M}_{app}=\begin{bmatrix}z(1-z^{-1})^{\alpha}\mathbf{I}-\mathbf{A}_{f1} & 0\\ 0 & z(1-z^{-1})^{\beta}\mathbf{I}-\mathbf{A}_{f2}\end{bmatrix}. \tag{26}$$

The output equation is given by

$$\begin{bmatrix}\mathbf{Y}_1\\ \mathbf{Y}_2\end{bmatrix}=\begin{bmatrix}\mathbf{C}_1 & 0\\ 0 & \mathbf{C}_2\end{bmatrix}\begin{bmatrix}\mathbf{X}_1\\ \mathbf{X}_2\end{bmatrix}. \tag{27}$$

3.5. Analysis. In the case of the interconnected systems (1) and (2) considered above, the calculation of the state vectors $\mathbf{X}_1$ and $\mathbf{X}_2$ involves inverting the matrix $\mathbf{M}$ (e.g., $\mathbf{M}_{cas}$, $\mathbf{M}_{fl}$, $\mathbf{M}_{par}$, $\mathbf{M}_{app}$) which has diagonal components of the type (9). The inverse matrix $\mathbf{M}^{-1}$ can be calculated as $\mathbf{M}^{D}/\det(\mathbf{M})$. The elements of the adjoint matrix $\mathbf{M}^{D}$ are of the form

$$\left[\mathbf{M}^{D}\right]_{ij}=\sum_{k=0}^{+\infty}\xi_{ijk}z^{-k+N+M-1}, \tag{28}$$

where

$$\det(\mathbf{M})=\sum_{k=0}^{+\infty}\zeta_k z^{-k+N+M}. \tag{29}$$

The upper summation limits in (28) and (29) are infinite. Hence, both the expressions are Laurent's series representations of analytic functions which are valid in the corresponding convergence regions.

Let us generalize the obtained results. In the case of more than two interconnected FO LTI systems, the state-space equation of such a system is of the form

$$\mathbf{MX}=\mathbf{F}, \tag{30}$$

where $\mathbf{M}$ is the matrix of elements being functions of the z-variable, $\mathbf{X}$ is the state vector and $\mathbf{F}$ is the input-related vector.

Solving this state-space equation still requires the inversion of the matrix $\mathbf{M}$ and calculation of $\det(\mathbf{M})$. The characteristic equation for such a system can be written as $f(z)=\det(\mathbf{M}(z))=0$.

4. Stability analysis of interconnected discrete-time FO LTI systems

The basic interconnections in the previous section can be extended towards other interconnection topologies including more than two systems. Assume that L is the length of practical implementation (Busłowicz and Ruszewski, 2013; Busłowicz, 2012; Kaczorek, 2008). Then, the upper limits of summations in (28) and (29) are replaced by L. Based on the results of Busłowicz and Ruszewski (2013), Busłowicz (2012), and Kaczorek (2008), we can introduce analogous definitions and theorems.

Definition 1. The system consisting of interconnected FO subsystems is called *practically stable* if the interconnected FO subsystems, each of the length L of the practical implementation, are asymptotically stable.

Definition 2. The system consisting of interconnected FO subsystems is called *asymptotically stable* if the interconnected FO subsystems, each of the length L of the practical implementation, are asymptotically stable for $L\to\infty$.

Theorem 2. (Ogata, 1987; Oppenheim *et al.*, 1999; Jury, 1964) *The discrete-time IO LTI system is asymptotically stable if and only if all zeros of the characteristic equation are strictly within the unit circle* $|z|<1$.

Theorem 3. *The system consisting of interconnected FO subsystems, each of the length L of practical implementation, is practically stable if and only if all zeros of the determinant* $\det(\mathbf{M})$ *are strictly within the unit circle* $|z|<1$.

Proof. For the finite length L, the elements of the matrix $\mathbf{M}^{-1}$ are rational functions of the z^{-1} variable with a common denominator being $\det(\mathbf{M})$. From Theorem 2, such a system is (asymptotically) stable if and only if all zeros of the denominator (i.e., the determinant $\det(\mathbf{M})$) are strictly within the unit circle $|z|<1$. ■

Corollary 1. *Assume that $L\to\infty$. Then, the system consisting of interconnected FO subsystems is asymptotically stable if and only if all zeros of* $\det(\mathbf{M})$ *are strictly within the unit circle* $|z|<1$.

Equivalently, to ensure the stability of the FO interconnected systems, the equation $f(z)=\det(\mathbf{M})=0$ cannot have any solution $z=z_i$ outside the unit circle. That is, the system is unstable if at least a single zero of $f(z)$ exists outside the unit circle. One can notice immediately that the stability of two interconnected systems guarantees the stability of their cascade, parallel and isolated interconnections. This is not true for the feedback interconnection. The stability of the system being an interconnection of FO systems cannot be evaluated based on its approximation with a finite length L of its practical implementation. This stems from the fact that zeros of the complex function of the complex variable may be unrelated to zeros of its finite-length approximation (i.e., polynomial or rational

approximation) (Delves and Lyness, 1967). For instance, the function $e(z) = e^z$ has no zeros whereas its finite-length polynomial approximations (i.e., $e(z) \approx \sum_{n=0}^{N} z^n/n!$) have N zeros. Furthermore, zero locations can be very sensitive to perturbations of coefficients of polynomial approximations (Wilkinson, 1994). To address these issues, we have developed a numerical test to evaluate stability of discrete-time systems described by non-polynomial characteristic equations.

5. Numerical test for stability evaluation

Stability evaluation requires knowledge about all zeros of the characteristic equation outside the unit circle $|z| > 1$. Such an area is infinite. Hence, the transformation

$$z = w^{-1} \tag{31}$$

is employed which maps the outer region of the unit circle to its inner region on the complex w-plane.

Corollary 2. *The interconnected systems are asymptotically stable if and only if there are no roots of the equation*

$$F(w) = 0, \tag{32}$$

where $F(w) = f(w^{-1})$, strictly within the unit circle $|w| < 1$.

Unfortunately, finding zeros of the complex-valued function of the complex variable is one of the oldest and still unsolved mathematical problems. For the purpose of stability evaluation, we adapt an innovative method of root finding applied in computational electromagnetics (Kowalczyk, 2018a). Although the proposed method is generic and easily implementable on computing machines, it evaluates stability of systems up to the limit of the assumed test resolution. The goal of the algorithm is to verify if any function zero exists and locate it by making use of Delaunay's triangulation (Weisstein, 2019b) of the unit circle on the complex plane. The accuracy of zero locations is controlled by the resolution parameter Δr. The algorithm is executed in the following steps:

Step 1. The unit circle on the complex w-plane is triangulated with a regular mesh, e.g., using Delaunay's triangulation. Two sets of nodes $W = \{w_1, w_2, \ldots, w_N\}$ and edges $E = \{e_1, e_2, \ldots, e_P\}$ are created. It is required that the length of the longest edge in E is less than or equal to the assumed test resolution Δr that controls the density of the triangular mesh.

Step 2. The phase quadrant in which the value of the function $F(w)$ lies is evaluated at all of the nodes $F = \{F(w_n) : w_n \in W\}$. In the proposed method, the complex value of the function is not required but only a quadrant in which its phase lies. Hence, the algorithm operates on four numbers associated with the complex-plane quadrants

$$Q(w_n) = \begin{cases} 1, & 0 \le \arg[f(w_n)] < \pi/2, \\ 2, & \pi/2 \le \arg[f(w_n)] < \pi, \\ 3, & \pi \le \arg[f(w_n)] < 3\pi/2, \\ 4, & 3\pi/2 \le \arg[f(w_n)] < 2\pi, \end{cases} \tag{33}$$

where $\arg[\cdot]$ denotes the principal argument of the complex number in the interval $[0, 2\pi)$. Therefore, the algorithm is not sensitive to the numerical precision of function-value computations.

Step 3. For each of the edges e_k between nodes w_p and w_q, the phase change is computed based on quadrants obtained in the previous step

$$\Delta Q(e_k) = Q(w_p) - Q(w_q). \tag{34}$$

Its value is from the set $\{-2, -1, 0, 1, 2\}$. Any zero or pole of the function $F(w)$ is a point where lines of quadrant-changes cross and regions meet for which the function values belong to four different quadrants. For instance, consider a function with a single zero $w = 0$ and a single pole $w = -0.5$ as presented in Fig. 2. The phase portrait of the function is placed in the background, i.e., the phase quadrants of function values are denoted by different colors. As seen, the zero and pole are located within the triangles 123. For a dense mesh, a zero/pole is located inside a triangle which has to include an edge such as $\Delta Q(e_k) = \pm 2$. This stems from the application of the triangular mesh in the algorithm. Of course, it would not be true for, e.g., a rectangular mesh. Hence, the vicinity of zero/pole of the considered function $F(w)$ can easily be detected, because it only requires to find all edges such that $\Delta Q(e_k) = \pm 2$. All these candidate edges are collected in a single set $E_c = \{e_k : \Delta Q(e_k) = \pm 2\}$. As can be seen, the zero/pole is a point around which the function values belong to each of the four different quadrants of the complex plane. However, directions of phase changes of the function (i.e., orders of color circulations) are opposite for zeros and poles. As can be seen, edges 13 are parts of two triangles 123 and 134, hence, the quadrangle 1234 is identified as a region of possible zero/pole location.

Step 4. The triangles including at least a single candidate edge from the set E_c, are collected in a single set of candidate triangles T_c. Then, all the edges of the triangles belonging to T_c are collected in the set E_t. Those edges that occur only once in E_t represent the boundary C of the candidate regions, because internal edges must be attached to two candidate triangles. The boundary C of the candidate regions is constructed only from the edges such as $|\Delta Q(e_k)| < 2$. Then, the set C is decomposed into subsets C_k, where C_k denotes a closed contour being

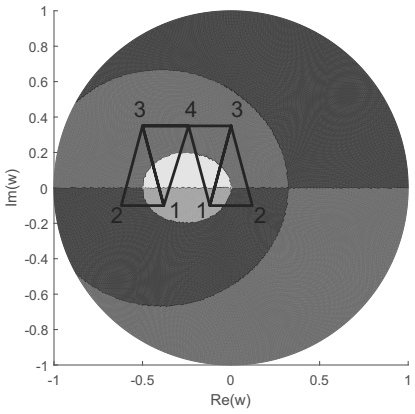

Fig. 2. Triangles around a single zero $w = 0$ and a single pole $w = -0.5$. For the candidate edges between nodes 1 and 3, $|\Delta Q| = 2$. Hence, zero/pole is potentially located inside the quadrangles 1234. Quadrants of the w-plane: $Q = 1$, $Q = 2$, $Q = 3$, $Q = 4$.

the boundary of the k-th candidate region. Starting from any edge from the set C, the algorithm searches for an edge connected to the considered one. Then, the process is repeated iteratively and the boundary of a region is constructed by finding the next edge connected to the previous one. Finally, if no edge is connected to the previous edge, the last edge should close the contour and the construction of the next candidate region can be started.

Step 5. The mesh is refined to increase the accuracy of locating zero/pole candidates. For this purpose, additional nodes are added in the centres of the edges in the candidate regions. Then, Delaunay's triangulation is executed to obtain a new mesh. Function $F(w)$ is evaluated at new nodes and the test starts from the second point for the locally denser mesh. The sizes of the candidate regions are smaller after the mesh refinement. Hence, the precision of zero/pole location is increased. The process of mesh refinement is repeated until the assumed precision of zero/pole location is obtained. During the mesh refinement, the problem of ill-conditioned mesh geometry (the so-called "skinny triangles") may appear (Kowalczyk, 2018a). To avoid this problem, an additional zone surrounding the region should be considered as recommended by Kowalczyk (2018a). Then, if the triangle is "skinny" in the extra zone (e.g., the ratio of the longest triangle edge to the shortest edge is greater than 3), a new additional node is added in its center.

Step 6. For each candidate region after the mesh refinement, Cauchy's argument principle (Weisstein, 2019a; Duren *et al.*, 1996; Krantz, 1999) is applied to its boundary contour C_k to verify the actual existence of a zero of the function $F(w)$ within this region. This step requires the evaluation of the parameter

$$q_k = \frac{1}{2\pi \mathrm{j}} \oint_{C_k} \frac{F'(w)}{F(w)} \, \mathrm{d}w \tag{35}$$

where $\mathrm{j} = \sqrt{-1}$. Based on Cauchy's argument principle, q_k is equal to the sum of all zeros counted with their multiplicities minus the sum of all poles counted also with their multiplicities within the contour C_k. If the region contains only a single candidate point, the value of q_k can be either a positive integer (zero of order q_k), a negative integer (pole of order $-q_k$), or zero (regular point). Equation (35) represents a total change in the argument of the function $F(w)$ over a closed contour C_k, which is given for the sampled function along the contour as

$$q_k = \frac{1}{2\pi} \sum_{p=1}^{P} \arg \left[\frac{F(w_{p+1})}{F(w_p)} \right], \tag{36}$$

where $w_1 = w_{P+1}$. We assume that points $\{w_k : k = 1, 2, \ldots, P\}$ belong to the contour C_k and the change in the function argument between two neighbouring points is always less than or equal to π.

Instead of directly using discrete Cauchy's argument principle (36), the value of q_k is computed for candidate regions by summing all the increases in the quadrants along the contour C_k in the counterclockwise direction

$$q_k = \frac{1}{4} \sum_{p=1}^{P} \Delta Q(e_p). \tag{37}$$

Finally, if any value of q_k is a positive integer, then a zero of $F(w)$ of order q_k is located and the system is unstable. If the method does not detect any zero within the unit circle, then the system is stable under limitation of the assumed test resolution Δr. For instance, if the distance between a single zero and a single pole on the complex w-plane is less than the assumed test resolution Δr, then the algorithm may not detect the system instability. However, any numerical computations aimed at evaluating stability are also always limited by the numerical precision, equal to 10^{-7} (single-precision floating-point format) or 10^{-16} (double-precision floating-point format).

6. Numerical results

We develop code for stability testing of interconnected FO systems in Matlab (Matlab, 2017). For this purpose, open source code of the global complex roots and poles finding algorithm based on phase analysis (Kowalczyk, 2018b) has been used as the starting point of our research. For numerical tests, we consider cascade, feedback and parallel interconnections of FO systems investigated by Stanislawski and Latawiec (2013b). The computations

are executed on an Intel Core i5-5200U processor clocked at 2.2 GHz. For the presented test results, the accuracy being the final candidate region size is set to $tol = 10^{-9}$. This parameter value is independent from the resolution parameter Δr which describes the initial maximum size of triangle edges in the mesh.

Let us consider the system S_1 $(\mathbf{A}_{f1}, \mathbf{B}_1, \mathbf{C}_1, \mathbf{D}_1)$ with $\alpha = 0.95$ given by the following matrices:

$$\mathbf{A}_{f1} = \begin{bmatrix} 0.6 & -1 \\ 1 & -1 \end{bmatrix}, \qquad \mathbf{B}_1 = \begin{bmatrix} 1 \\ 0 \end{bmatrix},$$
$$\mathbf{C}_1 = \begin{bmatrix} 1 & -0.95 \end{bmatrix}, \qquad \mathbf{D}_1 = 0. \tag{38}$$

The stability test of the system S_1 with the resolution $\Delta r = 0.01$ lasts $\Delta t = 6.965$ s and confirms that the system is stable. In Fig. 3, the final mesh obtained from the test execution is presented. As can be seen, the mesh is so dense that the phase portrait of the function is well visible. The algorithm finds the pole at $w = 0$ and verifies based on Cauchy's argument principle that it is the double pole without influence on the system stability. For $\Delta r = 0.1$, the stability test lasts $\Delta t = 0.926$ s and also confirms that the system is stable. Figure 4 shows that the mesh is only refined around the pole $w = 0$ whereas the other area of the unit circle is triangulated with edge sizes being maximally equal to $\Delta r = 0.1$. The computation time is below 1 s which demonstrates algorithm efficiency. However, any zero of $F(w)$ located at a distance less than $\Delta r = 0.1$ from the pole may not be detected by the algorithm. To sum up, reducing the accuracy of the test Δr results in longer execution times.

Consider the system S_2 $(\mathbf{A}_{f2}, \mathbf{B}_2, \mathbf{C}_2, \mathbf{D}_2)$ with $\alpha = 0.95$, given by the following matrices:

$$\mathbf{A}_{f2} = \begin{bmatrix} 0.8 & -1.17 \\ 1 & -1 \end{bmatrix}, \qquad \mathbf{B}_2 = \begin{bmatrix} 1 \\ 0 \end{bmatrix},$$
$$\mathbf{C}_2 = \begin{bmatrix} 1 & -1.05 \end{bmatrix} \qquad \mathbf{D}_2 = 0. \tag{39}$$

For the system S_2 and $\Delta r = 0.01$, the stability test lasts $\Delta t = 7.008$ s. The system is unstable, because there are conjugated zeros at $w = 0.799 \pm \mathrm{j}0.531$, cf. Fig. 5. It can be noticed that there is also a double pole in $w = 0$ and the order of color circulation around this point is opposite to the one for zeros at the phase portrait. For the system S_2 and $\Delta r = 0.1$, the stability test lasts $\Delta t = 0.954$ s. According to the test result, cf. Fig. 6, the system is unstable.

6.1. Cascade interconnection. For the cascade interconnection of the systems S_1 and S_2 and $\Delta r = 0.01$, the stability test lasts $\Delta t = 7.234$ s. Because one of the interconnected systems is unstable, the test should return that the interconnected system is also unstable. It is indeed confirmed by the test result because the system conjugated zeros are located at $w = 0.799 \pm \mathrm{j}0.531$ and the 4th order

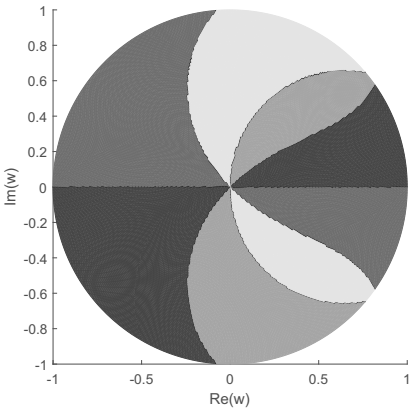

Fig. 3. Final mesh obtained for system S_1 after test execution with $\Delta r = 0.01$. Quadrants of the w-plane: ■ $Q = 1$, ■ $Q = 2$, ■ $Q = 3$, ■ $Q = 4$.

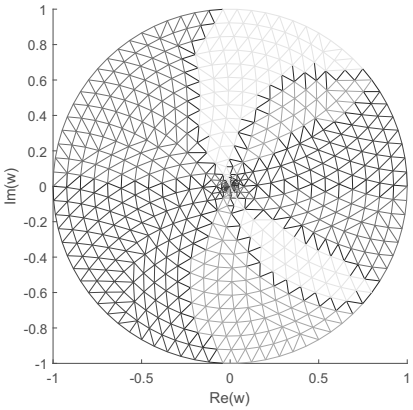

Fig. 4. Final mesh obtained for system S_1 after test execution with $\Delta r = 0.1$. Quadrants of the w-plane: ■ $Q = 1$, ■ $Q = 2$, ■ $Q = 3$, ■ $Q = 4$.

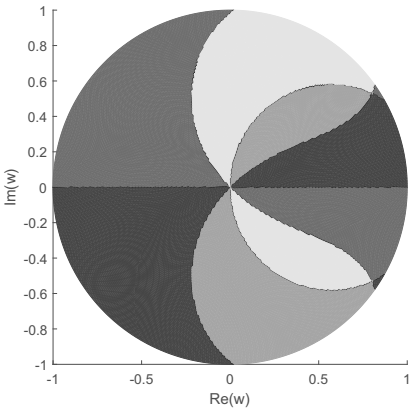

Fig. 5. Final mesh obtained for system S_2 after test execution with $\Delta r = 0.01$. Quadrants of the w-plane: ■ $Q = 1$, ■ $Q = 2$, ■ $Q = 3$, ■ $Q = 4$.

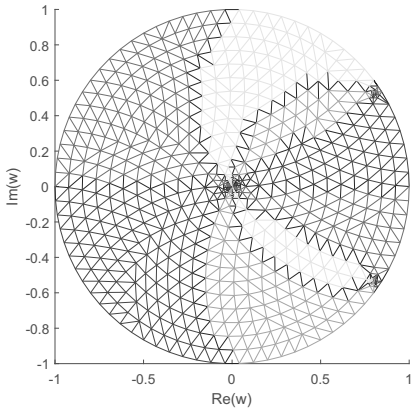

Fig. 6. Final mesh obtained for system S_2 after test execution with $\Delta r = 0.1$. Quadrants of the w-plane: ■ $Q = 1$, ■ $Q = 2$, ■ $Q = 3$, ■ $Q = 4$.

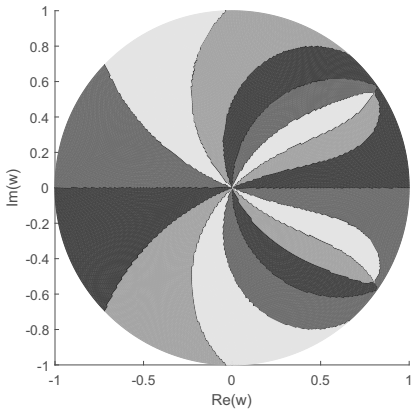

Fig. 7. Final mesh obtained for the cascade interconnection of systems S_1 and S_2 after test execution with $\Delta r = 0.01$. Quadrants of the w-plane: ■ $Q = 1$, ■ $Q = 2$, ■ $Q = 3$, ■ $Q = 4$.

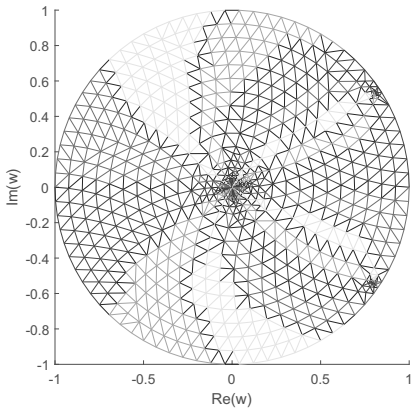

Fig. 8. Final mesh obtained for the cascade interconnection of systems S_1 and S_2 after test execution with $\Delta r = 0.1$. Quadrants of the w-plane: ■ $Q = 1$, ■ $Q = 2$, ■ $Q = 3$, ■ $Q = 4$.

pole is located at $w = 0$, cf. Fig. 7. For the cascade interconnection of systems S_1 and S_2 and $\Delta r = 0.1$, the stability test lasts $\Delta t = 0.745$ s. For these test parameters, the test also returns that the system is unstable, cf. Fig. 8.

6.2. Feedback interconnection. Consider the system S_3 $(\mathbf{A}_{f3}, \mathbf{B}_3, \mathbf{C}_3, \mathbf{D}_3)$ with $\alpha = 0.95$, given by the following matrices:

$$\begin{aligned}
\mathbf{A}_{f3} &= \begin{bmatrix} 1.56 & -2.536 & 0.96 \\ 1 & -1 & 0 \\ 0 & 1 & -1 \end{bmatrix}, \\
\mathbf{B}_3 &= \begin{bmatrix} 1 & 0.2 \\ 1 & -1.5 \\ -0.3 & 1 \end{bmatrix}, \\
\mathbf{C}_3 &= \begin{bmatrix} 0 & 1 & 0 \\ 1 & 0 & -0.6 \end{bmatrix}, \\
\mathbf{D}_3 &= \begin{bmatrix} 0 & 0 \\ 0 & 0 \end{bmatrix}.
\end{aligned} \tag{40}$$

Assume that the system S_3 is feedback interconnected with the system S_4 $(\mathbf{A}_{f4}, \mathbf{B}_4, \mathbf{C}_4, \mathbf{D}_4)$ with $\alpha = 0.84$ that is given by the following matrices:

$$\begin{aligned}
\mathbf{A}_{f4} &= \begin{bmatrix} 0.2 & -0.5121 \\ 1 & -1.1 \end{bmatrix}, & \mathbf{B}_4 &= \begin{bmatrix} 0.5 & 0 \\ 0 & 0.5 \end{bmatrix}, \\
\mathbf{C}_4 &= \begin{bmatrix} -0.5 & 0.5 \\ 0.5 & 0.5 \end{bmatrix}, & \mathbf{D}_4 &= \begin{bmatrix} 0 & 0 \\ 0 & 0 \end{bmatrix}.
\end{aligned} \tag{41}$$

Although both systems are stable separately, their feedback interconnection is unstable because there are conjugated zeros of the function $F(w)$ in the unit circle. In Fig. 9, one can notice these two single zeros at $w = 0.523 \pm \mathrm{j}0.283$ and the pole of the 5th order at $w = 0$. For the feedback interconnection of the systems S_3 and S_4 and $\Delta r = 0.01$, the stability test lasts $\Delta t = 7.285$ s.

6.3. Parallel interconnection. Let us consider the parallel interconnection of systems S_3 and S_4. In this case, the matrix $\mathbf{M}$ is block-diagonal and given by (24). Hence, if each of the interconnected systems is stable then their parallel interconnection is also stable. In Fig. 10, one can notice only the pole of the 5th order at $w = 0$. For the parallel interconnection of systems S_3 and S_4 and $\Delta r = 0.01$, the stability test lasts $\Delta t = 7.325$ s.

7. Conclusions

In this paper, we analyse the stability of interconnected discrete-time FO LTI state-space systems. We propose a general numerical test allowing us to evaluate the stability of interconnected systems. It consists of a transformation of the characteristic equation of the system, the triangulation of the unit circle with a

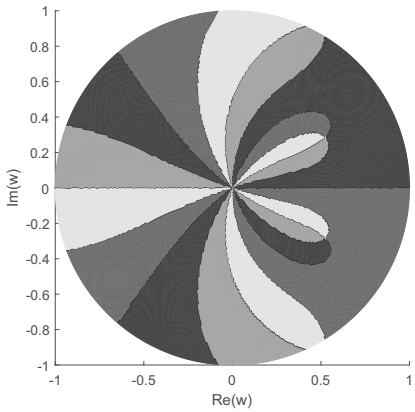

Fig. 9. Final mesh obtained for the feedback interconnection of systems S_3 and S_4 after test execution with $\Delta r = 0.01$. Quadrants of the w-plane: $Q = 1$, $Q = 2$, $Q = 3$, $Q = 4$.

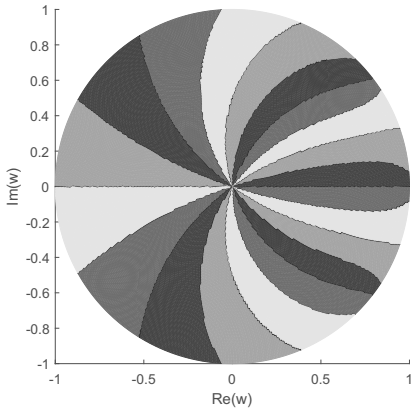

Fig. 10. Final mesh obtained for the parallel interconnection of systems S_3 and S_4 after test execution with $\Delta r = 0.01$. Quadrants of the w-plane: $Q = 1$, $Q = 2$, $Q = 3$, $Q = 4$.

self-adaptive mesh refinement and final verification based on Cauchy's argument principle. The test efficiency is demonstrated on several numerical tests for FO systems described by state-space equations.

Acknowledgment

The authors sincerely thank Prof. Zdzisław Kowalczuk for useful discussions and comments aimed at the improvement of the manuscript.

References

Bingi, K., Ibrahim, R., Karsiti, M.N., Hassam, S.M. and Harindran, V.R. (2019). Frequency response based curve fitting approximation of fractional-order PID controllers, *International Journal of Applied Mathematics and Computer Science* **29**(2): 311–326, DOI: 10.2478/amcs-2019-0023.

Brogan, W.L. (1991). *Modern Control Theory, 3rd Edn*, Prentice-Hall, Upper Saddle River, NJ.

Busłowicz, M. (2012). Simple analytic conditions for stability of fractional discrete-time linear systems with diagonal state matrix, *Bulletin of the Polish Academy of Sciences: Technical Sciences* **60**(4): 809–814.

Busłowicz, M. and Ruszewski, A. (2013). Necessary and sufficient conditions for stability of fractional discrete-time linear state-space systems, *Bulletin of the Polish Academy of Sciences: Technical Sciences* **61**(4): 779–786.

Busłowicz, M. and Kaczorek, T. (2009). Simple conditions for practical stability of positive fractional discrete-time linear systems, *International Journal of Applied Mathematics and Computer Science* **19**(2): 263–269, DOI: 10.2478/v10006-009-0022-6.

Delves, L.M. and Lyness, J.N. (1967). A numerical method for locating the zeros of an analytic function, *Mathematics of Computation* **21**: 543–560.

Duren, P., Hengartner, W. and Laugesen, R.S. (1996). The argument principle for harmonic functions, *The American Mathematical Monthly* **103**(5): 411–415.

Grzymkowski, L. and Stefański, T.P. (2018a). A new approach to stability evaluation of digital filters, *25th International Conference Mixed Design of Integrated Circuits and Systems (MIXDES), Gdynia, Poland*, pp. 351–354.

Grzymkowski, L. and Stefański, T.P. (2018b). Numerical test for stability evaluation of discrete-time systems, *23rd International Conference on Methods Models in Automation Robotics (MMAR), Międzyzdroje, Poland*, pp. 803–808.

Jury, E.I. (1964). *Theory and Application of the Z-Transform Method*, Wiley, New York, NY.

Kaczorek, T. (2008). Practical stability of positive fractional discrete-time linear systems, *Bulletin of the Polish Academy of Sciences: Technical Sciences* **56**(4): 313–317.

Kaczorek, T. and Ruszewski, A. (2020). Application of the Drazin inverse to the analysis of pointwise completeness and pointwise degeneracy of descriptor fractional linear continuous-time systems, *International Journal of Applied Mathematics and Computer Science* **30**(2): 219–223, DOI: 10.34768/amcs-2020-0017.

Kowalczyk, P. (2018a). Global complex roots and poles finding algorithm based on phase analysis for propagation and radiation problems, *IEEE Transactions on Antennas and Propagation* **66**(12): 7198–7205.

Kowalczyk, P. (2018b). GRPF: Global complex roots and poles finding algorithm, `https://github.com/PioKow/GRPF`.

Krantz, S.G. (1999). *Handbook of Complex Variables, 1st Edn*, Birkhäuser, Boston, MA.

Matlab (2017). *Matlab: User's Guide*, *Version 9.2.0 (R2017a)*, The MathWorks Inc., Natick, MA.

Mercorelli, P. (2017a). Combining flatness based feedforward action with a fractional PI regulator to control the intake valve engine, *18th International Carpathian Control Conference (ICCC), Sinaia, Romania*, pp. 456–461.

Mercorelli, P. (2017b). A discrete-time fractional order PI controller for a three phase synchronous motor using an optimal loop shaping approach, *in* A. Babiarz *et al.* (Eds), *Theory and Applications of Non-Integer Order Systems*, Springer, Cham, pp. 477–487.

Mozyrska, D. and Girejko, E. (2013). Overview of fractional h-difference operators, *in* A. Almeida, *et al.* (Eds), *Advances in Harmonic Analysis and Operator Theory*, Springer, Basel, pp. 253–268.

Ogata, K. (1987). *Discrete-Time Control Systems*, Prentice-Hall, Upper Saddle River, NJ.

Oppenheim, A.V., Schafer, R.W. and Buck, J.R. (1999). *Discrete-Time Signal Processing, 2nd Edn*, Prentice-Hall, Upper Saddle River, NJ.

Ostalczyk, P. (2012). Equivalent descriptions of a discrete-time fractional-order linear system and its stability domains, *International Journal of Applied Mathematics and Computer Science* **22**(3): 533–538, DOI: 10.2478/v10006-012-0040-7.

Samko, S.G., Kilbas, A.A. and Marichev, O.I. (1993). *Fractional Integrals and Derivatives: Theory and Applications*, Gordon and Breach, New York, NY.

Stanislawski, R. and Latawiec, K. (2013a). Stability analysis for discrete-time fractional-order LTI state-space systems. Part I: New necessary and sufficient conditions for the asymptotic stability, *Bulletin of the Polish Academy of Sciences: Technical Sciences* **61**(2): 353–361.

Stanislawski, R. and Latawiec, K. (2013b). Stability analysis for discrete-time fractional-order LTI state-space systems. Part II: New stability criterion for FD-based systems, *Bulletin of the Polish Academy of Sciences: Technical Sciences* **61**(2): 363–370.

Vaccaro, R.J. (1995). *Digital Control, 1st Edn*, McGraw-Hill, New York, NY.

Weisstein, E.W. (2019a). Argument principle, *Mathworld—A Wolfram Web Resource*, `http://mathworld.wolfram.com/ArgumentPrinciple.html`.

Weisstein, E.W. (2019b). Delaunay triangulation, *Mathworld—A Wolfram Web Resource*, `http://mathworld.wolfram.com/DelaunayTriangulation.html`.

Wilkinson, J.H. (1994). *Rounding Errors in Algebraic Processes*, Dover, New York, NY.

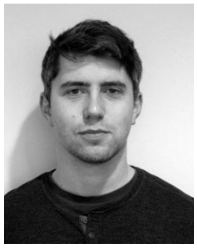

Łukasz Grzymkowski obtained his MSc degree in robotics and automation from the Gdańsk University of Technology (GUT) in 2014, with the focus on state estimation of mobile robots using Kalman filtering. He is currently pursuing his PhD degree in the Department of Decision Systems and Robotics at the Faculty of Electronics, Telecommunications and Informatics of the GUT. His work investigates modern methods and applications of stability analysis.

Damian Trofimowicz received his MSc degree in electronics engineering from the Gdańsk University of Technology (GUT) in 2009. In 2011, he also obtained an MSc degree at the GUT in the field of management and economics. In 2011–2015, he was a part of the RF Design team in the Vector company placed in Gdynia, Poland, developing RF amplifiers and optical nodes. In 2015, he joined the Microwave Design Department in the Spaceforest company located in Gdynia, where he is involved in the development of microwave oscillators, amplifiers and other devices dedicated for space environment. He conducts research on semiconductor modelling and optimization.

Tomasz P. Stefański received his MSc degree in telecommunications and his PhD degree in electronics engineering from the Gdańsk University of Technology (GUT), Poland, in 2002 and 2007, respectively. He is currently an associate professor at the Faculty of Electronics, Telecommunications and Informatics at the GUT. Before joining the university in 2011, he was with the Swiss Federal Institute of Technology (ETH Zurich), conducting research on parallelization of electromagnetic solvers on modern computing architectures using the OpenCL programming language. Between 2006 and 2009 he worked at the University of Glasgow, developing parallel alternating direction implicit finite-difference time-domain (ADI-FDTD) full-wave solvers for general purpose high-performance computers and graphics processing units. His current research interests include parallel processing, computational electromagnetics and scientific computing.

Received: 21 January 2020
Revised: 22 April 2020
Accepted: 7 June 2020